Short Communication

Study on MXene-supported Layered TiS₂ as Cathode Materials for Magnesium Batteries

Yuan Li, Donghui Xu, Dehang Zhang, Yuanchi Wei, Dianli Qu, Yuxiang Guo[*]

School of High Temperature Materials and Magnesium Resources Engineering,
University of Science and Technology Liaoning, Anshan, 114051, China
[*]E-mail: gyxwsd@126.com

TiS₂/MXene composites with different molar ratio were successfully prepared by one-step hydrothermal method, and the optimal proportion was confirmed by characterization. The electrochemical performance of TiS₂/MXene composite and TiS₂ as magnesium battery cathode were tested. The test results show that at the current density of 50 mA/g, TiS₂/MXene composite exhibits enhanced capacities of 97 mAh/g. Compared with pure TiS₂, it has higher charge-discharge capacity and better cycle performance. At the same time, the introduction of new MXene materials also provides a new idea for the study of new anode materials for magnesium batteries.

1. INTRODUCTION

With the application of various high technologies and the improvement of people's living standards, the demand for batteries in the market is increasing. How to make batteries with efficient energy conversion and storage has become a worldwide research topic [1-3]. At present, lithium batteries are most widely studied and commonly used, but there are serious safety and environmental pollution problems in the process of charging and discharging [4-6]. Therefore, it is extremely urgent to research and develop a new type of clean and environmentally friendly energy sources [7]. As the diagonal elements on periodic table of elements, magnesium and lithium have similar physical and chemical properties. Compared with lithium, magnesium is abundant in the crust and cheaper, It is easy to process and also safer [8-11]. So, magnesium batteries have a good development prospect to be used as negative electrode [12].

Composed of magnesium negative electrode, the working principal of electrolyte and cathode material and the magnesium ion battery is similar to that of lithium ion battery. Magnesium ions are

reversibly deposited/dissolved at the negative electrode and reversibly embedded/detached at the positive electrode [13-17]. At present, the research on magnesium ion battery is still in the preliminary stage, sothere are a lot of problems to be solved urgently [18-20]. On the one hand, a layer of purified film will be formed on the surface in most of the solution because magnesium is more active. [21] It is difficult for divalent magnesium ions to pass through this passive film, making it hard for magnesium to dissolve and deposit, and thus limiting the electrochemical activity of magnesium. [22] On the other hand, the divalent magnesium ion has small volume, large electric density and strong polarization ability, so there are few substrate materials for rapid embedding of magnesium ions [23-24]. Cathode materials are the key factor restricting the development of magnesium batteries. But in the existing study, there are some problems in the process of charging and discharging of these cathode materials, such as Mg^{2+} diffusion, poor conductivity and poor compatibility with electrolyte. Many domestic and foreign scholars are committed to find and develop new cathode materials [25].

As the cathode materials for magnesium ion batteries, transition metal sulfides not only have great research potential, but also are considered as the typical embedding and detaching material [37-38]. TiS_2 is one of the transition metal sulfides which are most commonly studied. TiS_2 is in layered structure formed by S-M-S lamellae, so ions can be inserted into the gap between the lamellae[49]. Various researches on TiS_2 as cathode material for magnesium batteries show that TiS_2 can achieve the reversible de-embedding of magnesium ions, but the capacity degradation is serious[50-52]. In order to improve the detaching of magnesium ions in TiS_2 substrate materials, MXene, which is a graphene-like layered compound with excellent conductivity, is used. MXene is a general term for a new type of two-dimensional layered compound with a graphene-like structure. The chemical formula is $M_{n+1}X_nT_x$ (n=1, 2,3, of which M is a transition metal element; X is a carbon or nitrogen, and T_x is the surface group, such as O^{2-}, OH^-, F^-, NH_3, NH^{4+}) [53-55]. MXene has good conductivity and hydrophilia, which makes it an ideal substrate material for supporting active TiS_2. As far as we know, there is no report on TiS_2/MXene composites as cathode materials for magnesium batteries.

In this paper, TiS_2/MXene-Ti_3C_2 composites with different molar ratios are prepared by one-step hydrothermal method, and the optimal ratio is selected as the cathode material for magnesium batteries. Compared with pure TiS_2 cathode material, TiS_2/MXene-Ti_3C_2 composite shows a build-up capacity of 97mAh/g at 50mA/g.

2. EXPERIMENT

2.1 Preparation of TiS₂/MXene Composite

Firstly, TiS_2 and MXene-Ti_3C_2 were accurately weighed in molar ratios of 1:2, 1:1 and 2:1 respectively. Then MXene-Ti_3C_2 was dispersed in 70mL distilled water, and ultrasonic dispersion was conducted for 30 minutes. After being dispersed uniformly, TiS_2 was added and fully stirred for 3 hours to be mixed evenly. Then the mixed solution was transferred to 100mL stainless steel autoclave, and was kept at 190 °C for 24 hours. After cooling to the room temperature, the autoclave was alternately and centrifugally washed five times with distilled water and alcohol. At last, the sediment

was dried in vacuum at 120 °C for 15 hours to obtain TiS_2/MXene-Ti_3C_2 composite.

In general, the pure two-dimensional material, MXene-Ti_3C_2 is prepared by immersing Ti_3AlC_2 in the mixture of diluted hydrochloric acid and lithium fluoride [56-59]. And TiS_2 was purchased from China Leshan Koyada Photoelectric Technology Company.

2.2 Material Characterization

X' Pert Powder X-ray diffractometer (Cu Target Kal radiation, current: 40 mA, voltage: 40 kV, scanning speed: 4° /min, scanning angle: $2\theta=10°\sim90°$) was used to deal with the phase analysis towards the sample. Microstructure and morphology of the prepared samples were observed by HD field emission scanning electron microscopy (SEM).

2.3. Test of Electrochemical Performance

Active materials, conductive black and PVDF were dispersed in the N-methyl-2-pyrrolidone (NMP) at a mass ratio of 8:1:1. The slurry after fully grinding was evenly coated on the copper foil. The electrode material was dried at 110 °C in the vacuum oven for 12 hours and then put it on the powder compressing machine for tablet compressing. The quality before and after coating the copper foil was weighed and the mass of active material was calculated. After all these steps, the electrode material was put into the glove box for use. In the glove box, the CR2032 button battery was assembled from bottom to top according to the sequence of negative shell, magnesium sheet, electrolyte (APC), fiberglass diaphragm, electrolyte, positive electrode, gasket, spring sheet and positive shell. Then pressed and sealed it. The sealed battery would be tested for its electrochemical performance after standing for 6 hours. The charge-discharge test was carried out on the LAND battery test system. The test temperature was 25 °C and the cut-off voltage was 0.01~2.0V (vs. Mg/Mg^{2+}).

3. RESULTS AND DISCUSSION

3.1 XRD and SEM Analysis

Figure 1 shows the XRD spectrum of TiS_2, MXene-Ti_3C_2 and TiS_2/MXene-Ti_3C_2 composite with different molar ratios and the standard spectrum of TiS_2. According to the XRD spectrum of TiS_2 in the figure, it can be observed that a series of diffraction peaks at 15.57°, 34.21°, 44.15°, 53.78°, 57.69°, and 65.47° are corresponding to (001), (011), (102), (110), (103) and (004) crystal planes, which matches with the standard card (JCPDS 03-065-3369)[50-52]. No impure peak appears. The XRD diffraction spectrum of pureMXene-Ti_3C_2 shows that the main absorption peak is located at $2\theta=18.22°$, 26.97°, 33.89°, 52.69° and 60.5°, respectively corresponding to (006), (008), (010), (012) and (110) crystal planes, which is consistent with the results in other literature reports[60-62]. In the XRD spectrum of TiS_2/MXene-Ti_3C_2 composite, all the diffraction peaks are consistent with the

diffraction peaks of TiS_2 and MXene-Ti_3C_2, indicating that the prepared MXene-Ti_3C_2 is a coexisting phase of TiS_2 and MXene-Ti_3C_2 , and the nanocomposite is successfully prepared. The diffraction peaks of 33.89°, 52.60° and 60.5° identified by squares are due to the increase in the molar ratio of TiS_2 and MXene-Ti_3C_2, and the three diffraction peaks show a regular change. With the increase of molar ratio, the diffraction peak of MXene-Ti_3C_2 in the composite increases gradually, indicating that MXene-Ti_3C_2 nano lamella is well separated, rather than stacked together.

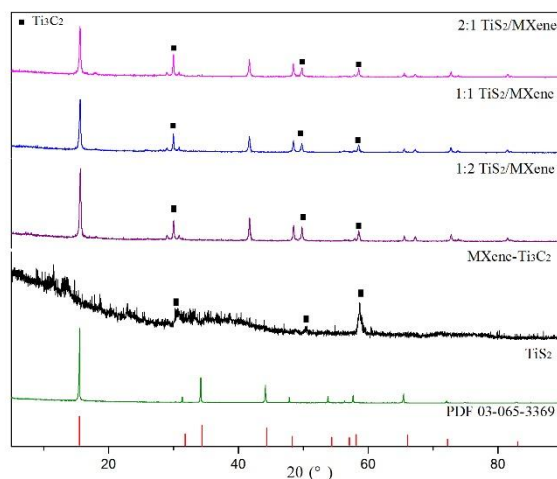**Figure 1.** XRD Spectrum of TiS_2, MXene-Ti_3C_2 and TiS_2/MXene-Ti_3C_2 Composite with Different Molar Ratios

Figure 2 is the SEM image of TiS_2, MXene-Ti_3C_2 and TiS_2/MXene-Ti_3C_2 composite with different molar ratios at different multiples. Figure 2(a) shows the SEM picture of pure TiS_2, from which we can see that TiS_2 presents an irregular lamellar shape]. Figure 2(b) shows us the MXene-Ti_3C_2. It can be seen that MXene-Ti_3C_2 has an organ-shaped layered structure. The layers with smooth surface are separated from each other. Figure 2(c-e) is the SEM images of TiS_2/MXene-Ti_3C_2 composite with molar ratios of 1:2, 1:1 and 2:1, from which we can see that pure TiS_2's appearance on MXene-Ti_3C_2 layered material is different from its original appearance. MXene-Ti_3C_2 layer provides more active sites for TiS_2, making TiS_2 distribution more uniform. TiS_2 nano-particles are supported on the surface and between the layer gap of the two-dimensional layered MXene-Ti_3C_2, increasing the layer spacing and specific surface area. From Figure 2(c-d), we can see that TiS_2 is heavily stacked and covering the layer of MXene-Ti_3C_2 , which is not conducive to ion insertion and separation. According to Figure 2(e), TiS_2 is uniformly dispersed on the MXene-Ti_3C_2 lamellar layer to support MXene-Ti_3C_2 lamellar structure, inhibiting the collapse of the lamellar layer, and facilitating the entry of ions into the layer.

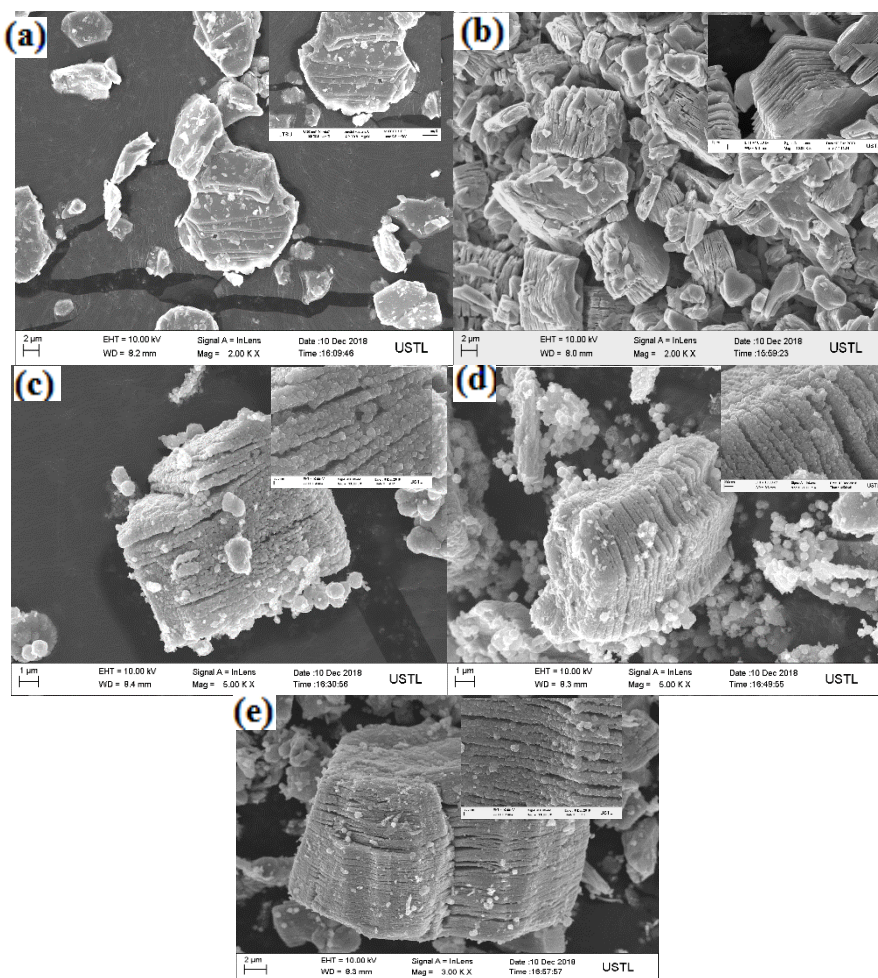**Figure 2.** SEM Image of TiS_2, MXene-Ti_3C_2 and TiS_2/MXene-Ti_3C_2 Composite with Different Molar Ratios at Different Multiples
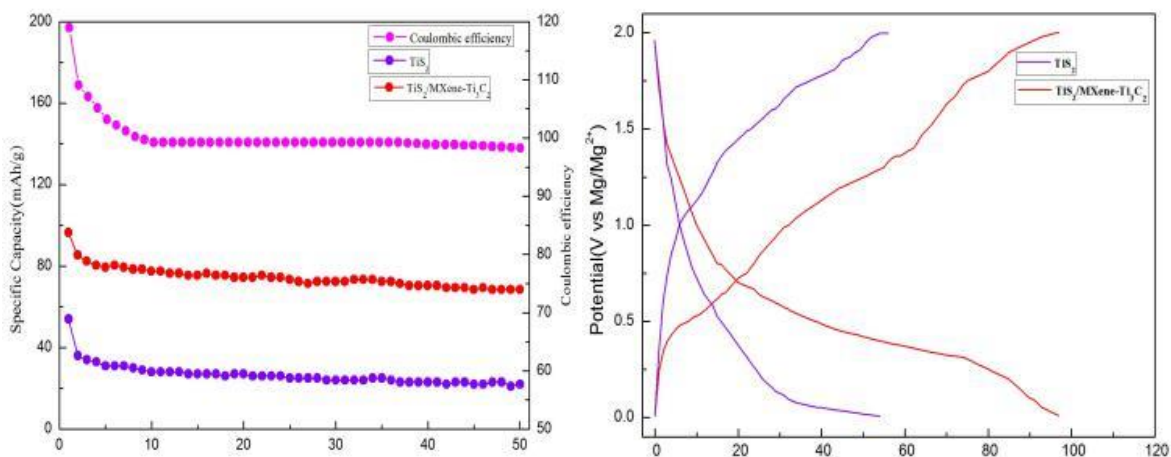
3.2 Analysis of Electrochemical Performance

Figure 3. Cycle Performance Chart (a) and Charge-Discharge Curve (b) of TiS_2 and TiS_2/MXene-Ti_3C_2 Composite with Molar Ratio of 2:1

Figure 3(a) and (b) show us the cycle performance and charge-discharge curves of TiS_2 and $TiS_2/MXene-Ti_3C_2$ composite with a molar ratio of 2:1 (0.1V-2.0V). When the electrolyte is APC, TiS_2 has a capacity of only 58mAh/g at a current density of 50 mA/g, while $TiS_2/MXeneMXene-Ti_3C_2$ composite has a capacity of 97mAh/g. After 50 cycles, its capacity becomes 75mAh/g, and the capacity fading is not serious. The first charge-discharge capacity of the composite is obviously higher than that of TiS_2 in the voltage range of 0.1V-2.0V.

Table 1. Comparison with other cathode materials of magnesium battery.

Cathode material	Electrolyte	Capacity (mAh/g)	References
V_2O_5	$Mg(ClO_4)_2$/THF	50	[26-30]
$Mg_xV_2O_5$	Acetonitrile	250	[31]
Mo_6S_8	Magnesium organo-haloaluminate complex electrolyte	130	[32-33]
MoS_2	$Mg(AlClBu)_2$/THF	22	[34-36]
TiS_2	Dibutyl magnesium electrolyte	36	[37-39]
MoO_3	$MgCl_2$/EMIC/$AlCl_3$ salt melt	160	[40-42]
MnO_2(Hollandite)	$Mg(ClO_4)_2$/AC	85	[43-44]
MnO_2 (Birnessite)	$Mg(ClO_4)_2$	65	[45-47]
MnO_2 (Spinel)	$Mg(ClO_4)_2$	80	[48]
TiS_2	APC	58	In this paper
$TiS_2/MXene-Ti_3C_2$	APC	97	In this paper

Table 1 shows many studies about transition metal oxide and sulfide as positive electrode of magnesium battery. Compared with the cathode material shown in Table 1 above, when the electrolyte is APC, the charge-discharge capacity of pure TiS_2 have been greatly improved. With the addition of $MXene-Ti_3C_2$, the storage capacity of magnesium ions has been improved. This is because $MXene-Ti_3C_2$ nanosheet with good conductivity provides a looser structure for the entry and exit of magnesium ions, thus providing more active sites for the storage of magnesium ions, and shortening the diffusion path of magnesium ions. Both coulombic efficiencies are close to 100%.

4. CONCLUSION

In conclusion, $TiS_2/MXene-Ti_3C_2$ composite has been successfully prepared by one-step hydrothermal method. The addition of $MXene-Ti_3C_2$ with high conductivity and large specific surface area is conductive to the embedding/detaching of magnesium ions. And the effect is more obvious when the molar ratio of TiS_2 to MXene is 2:1. Compared with pure TiS_2, $TiS_2/MXene-Ti_3C_2$ composite has higher reversible capacity of 97mAh/g and better cycle performance at the condition of 50mA/g.

CONFLICTS INTEREST
There are no conflicts to declare.

References

1. M. Wang, F. Zhang, and C.S. Lee, *Adv. Energy Mater*., 7 (2017) 1700536.
2. J. Cui, T.G. Zhan, and K.D. Zhang, *Chin. Chem. Lett.,* 28 (2017) 2171.
3. P. Novák, R. Imhof, and O. Haas, *Electrochim. Acta*, 45 (1999) 351.
4. D. Aurbach, Z. Lu, and A. Schechter, *Nature,* 407 (2000) 724.
5. D. Aurbach, G.S. Suresh and E. Levi, *Adv. Mater*., 19 (2007) 4260.
6. L. Wang, B. Jiang, and P.E. Vullum, *ACS nano*, 12 (2018) 2998.
7. H.D. Yoo, I. Shterenberg, Y. Gofer, G. Gershinsky, N. Pour, and D. Aurbach, *Energy Environ. Sci.*, 6 (2013) 2265.
8. P. Saha, M.K. Datta, O.I. Velikokhatnyi, A. Manivannan, D. Alman, and P.N. Kumta, *Prog. Mater. Sci.*, 66 (2014) 1.
9. J.B. Goodenough and Y. Kim, *Chem. Mater*., 22 (2010) 587.
10. E. Levi, Y. Gofer, and D. Aurbach, *Chem. Mater*., 22 (2010) 860.
11. W. Jin, Z.G. Wang, and Y.Q. Fu, *J. Mater. Sci.,* 51 (2016) 7355.
12. Z. Wang , Q. Su, abd H. Deng, *Phys. Chem. Chem. Phys*., 15 (2013) 8705.
13. L. Wang, Z. Wang, and P.E. Vullum, *Nano lett*., 18 (2018) 763.
14. M.M. Huie, D.C. Bock, and E.S. Takeuchi, *Coord. Chem. Rev*., 287 (2015).
15. Q. An, Y. Li, and H.D. Yoo, *Nano Energy*, 18 (2015) 265.
16. Y. Liang, R. Feng, and S. Yang, *Adv. Mater*., 23 (2011) 640.
17. M. Xu, S. Lei, and J. Qi, *ACS Nano*, 112 (2018) 3733.
18. E. Levi, A. Mitelman, D. Aurbach, and M. Brunelli, *Chem. Mater*., 19 (2007) 5131.
19. B. Peng, J. Liang, Z. Tao, and J. Chen, *J. Mater. Chem*. A, 19 (2009) 2877.
20. E. Levi, G. Gershinsky, D. Aurbach, and O. Isnard, *Inorg. Chem*., 48 (2009) 8751.
21. E. Levi, Y. Gofer, and D. Aurbach, *Chem. Mater*., 22 (2010) 860.
22. R.E. Bell and R.E. Herfert, *Am. Chem. Sci. J*., 79 (1957) 3351.
23. J. Whitacre, A. Tevar, and S. Sharma, *Electrochem. Commun*., 12 (2010) 463.
24. X. Zhou, R.K. Guduru, and P. Mohanty, *J. Mater. Chem*. A, 1 (2013) 2757.
25. O. Chusid, Y. Gofer, H. Gizbar, Y. Vestfrid, E. Levi, D. Aurbach, and I. Reich, *Adv. Mater*.,15 (2003) 627.
26. L. Yu and X. Zhang, *J. Colloid Interface Sci*., 278 (2004) 160.
27. P.E. Tang, J.S. Sakamoto, E. Baudrin and B. Dunn, *J. Non-Cryst. Solids*, 350 (2004).
28. I. Stojkovic, N. Cvjeticanin, S. Markovic, M. Mitric and S. Mentus, *Acta Phys. Pol.* A, 117 (2010) 837.
29. V. Shklover, T. Haibach, F. Ried, R. Nesper and P. Novak, J. *Solid State Chem*., 123 (1996) 317.
30. J.P. Pereira-Ramos, R. Messina and J. Perichon, *J. Electroanal. Chem*., 218 (1987) 241.
31. S.H. Lee, R.A. DiLeo, A.C. Marschilok, K.J. Takeuc and E.S. Takeuchi, *ECS Electrochem. Lett*. 3 (2014) A87.
32. P. Novak and J. Desilvestro, *J. Electrochem. Soc*., 140 (1993) 140.
33. Y. Liu, L. Jiao, Q. Wu, J. Du, Y. Zhao, Y. Si, Y. Wang, and H. Yuan, *J. Mater. Chem. A,* 1 (2013)

5822.

34. Y. Liu, L. Jiao, Q. Wu, Y. Zhao, K. Cao, H. Liu, Y. Wang, and H. Yuan, *Nanoscale*, 5 (2013) 9562.
35. S. Yang, D. Li, T. Zhang, and Z. Tao, *J. Phys. Chem*. C, 116 (2012) 1307.
36. Y. Liang, R. Feng, S. Yang, H. Ma, and J. Liang, *J. Chen, Adv. Mater*., 23 (2011) 640.
37. P.G. Bruce, F. Erok, and J. Nowinski, *J. Mater. Chem*., 1 (1991) 705.
38. P.G. Bruce, F. Erok, and P. Lightfoot, *Solid State Ionics*, 53 (1992) 351.
39. P. Lightfoot, F. Erok, and J.L. Nowinski, *J. Mater. Chem*. A, 2 (1992) 139.
40. H.W. Wang, M. Naguib, K. Page, D.J. Wesolowski and Y. Gogotsi, *Chem. Mater*., 28 (2015) 349.
41. J. Halim, K.M. Cook, M. Naguib, P. Eklund, Y. Gogotsi, J. Rosen and M.W. Barsoum, *Appl. Surf. Sci.,* 362 (2016) 406.
42. Y. Ying, Y. Liu, X. Wang, Y. Mao, W. Cao, P. Hu and X. Peng, *ACS Appl. Mater. Interfaces*, 7 (2015) 1795.
43. M. Naguib, J. Come, B. Dyatkin, V. Presser, P.L. Taberna, P. Simon, M.W. Barsoum and Y. Gogotsi, *Electrochem. Commun*., 16 (2012) 61.
44. Z. Lin, D. Sun, Q. Huan, J. Yang, M.W. Barsoum and X. Yan, *J. Mater. Chem.* A, 3 (2015) 14096.
45. F. Shahzad, M. Alhabeb, C.B. Hatter, B. Anasori, S.M. Hong, C.M. Koo and Y. Gogotsi, *Science,* 353 (2016) 1137.
46. Y. Qing, W. Zhou, F. Luo and D. Zhu, *Ceram. Int*., 42 (2016) 16412.
47. M. Nath and C.N.R. Rao, *Angew. Chem., Int. Ed*., 41 (2002) 3451.
48. J. Chen, Z.L. Tao and S.L. Li, Angew. *Chem., Int. Ed*., 42 (2003) 2147.
49. J. Chen, S.L. Li, Z.L. Tao, Y.T. Shen and C.X. Cui, *J. Am. Chem. Soc*., 125 (2003) 5284.
50. L. Lu, X. Han, J. Li, J. Hua and M.O Yang, *J Power Sources*, 226 (2013) 272.
51. J. Xie, X.Wang and A. LI, *Corros. Sci*., 60 (2012) 129.
52. M. Nguib, V. Presser and N. Lane, *RSC Adv*., 1 (2011) 1493.
53. M. Kurtoglu, M. Naguib and Y. Gogotsi, *MRS Commun*., 1 (2012) 1.
54. H.W. Wang, M. Naguib, K. Page, D.J. Wesolowski and Y. Gogotsi, *Chem. Mater*., 28 (2015) 349.
55. Y. Ying, Y. Liu, X. Wang, Y. Mao, W. Cao, P. Hu and X. Peng, *ACS Appl. Mater. Interfaces*, 7 (2015) 1795.
56. M. Naguib, J. Come, B. Dyatkin, V. Presser, P.L. Taberna, P. Simon, M.W. Barsoum and Y. Gogotsi, *Electrochem. Commun*., 16 (2012) 61.
57. Z. Lin, D. Sun, Q. Huang, J. Yang, M.W. Barsoum and X. Yan, *J. Mater. Chem*. A, 3 (2015) 14096.
58. X. Wang, S. Kajiyama, H. Iinuma, E. Hosono, S. Oro, I. Moriguchi, M. Okubo and A. Yamada, *Nat. Commun*., 6 (2015) 1.
59. F. Shahzad, M. Alhabeb, C.B. Hatter, B. Anasori, S.M. Hong, C.M. Koo and Y. Gogotsi, *Science*, 353 (2016) 1137.
60. C.E. Ren, K.B. Hatzell, M. Alhabeb, Z. Ling, K.A. Mahmoud and Y. Gogotsi, *J. Phys. Chem. Lett*., 6 (2015) 4026.
61. J. Chen, K. Chen, D. Tong, Y. Huang, J. Zhang, J. Xue, Q. Huang and T. Chen, 51 (2015) 314.
62. J. Luo, W. Zhang, H. Yuan, C. Jin, L. Zhang, H. Huang, C. Liang, Y. Xia, J. Zhang, Y. Gan and X. Tao, *ACS Nano*, 11 (2017) 2459.